JOURNAL OF GEOPHYSICAL RESEARCH, VOL. 106, NO. D18, PAGES 20,913–20,924, SEPTEMBER 27, 2001

Ground-based measurements of tropospheric CO, C_2H_6, and HCN from Australia at 34°S latitude during 1997–1998

Curtis P. Rinsland
NASA Langley Research Center, Hampton, Virginia, USA

Arndt Meier and David W. T. Griffith
Department of Chemistry, University of Wollongong, Wollongong, New South Wales, Australia

Linda S. Chiou
Wyle Laboratories, Hampton, Virginia, USA

Abstract. High spectral resolution (0.004 cm^{-1}) infrared solar absorption measurements of CO, C_2H_6, and HCN have been recorded with the Fourier transform spectrometer located at the Network for the Detection of Stratospheric Change complementary station at the University of Wollongong, Australia (34.45°S, 150.88°E, 30 m above sea level). The time series covers March 1997 to February 1998. Profile retrievals with maximum sensitivity in the upper troposphere show distinct seasonal cycles for all three molecules with maxima during October–December 1997. Best fits to the time series of daily averages yield peak 0.03–14 km columns (molecules cm^{-2}) of 1.54×10^{18} for CO, 8.56×10^{15} for C_2H_6, and 6.56×10^{15} for HCN during austral spring. Mixing ratio profiles of all three molecules during this time show maxima in the upper troposphere. Isentropic back trajectories suggest the elevated CO, C_2H_6, and HCN columns above Wollongong originated from southern Africa or South America with no significant contribution from the intense tropical Asian emissions during the strong El Niño event of 1997–1998.

1. Introduction

In this paper we report and interpret a time series of CO, C_2H_6, and HCN vertical profile measurements with maximum sensitivity in the upper troposphere. The observations were obtained between March 1997 and February 1998 at the University of Wollongong, Australia (34.45°S, 150.88°E, 30 m above sea level (asl)). The three molecules selected for analysis have infrared absorption features that are sufficiently strong that they may be measured globally from such spectra and are important indicators of tropospheric pollution and transport. Southern hemispheric emissions of these molecules result almost entirely from tropical biomass burning [e.g., *Watson et al.*, 1990; *Fishman et al.*, 1991; *Rudolph*, 1995; *Li et al.*, 2000]. Lesser emission sources in the southern hemisphere include in situ production of CO from CH_4 nonmethane hydrocarbon oxidation during transport, and oceanic emissions of C_2H_6 [e.g., *Rudolph*, 1995; *Manning et al.*, 1997].

Enhanced middle and upper tropospheric columns of these molecules may originate from multiple tropical source regions because of their relatively long lifetimes (global lifetime of 2 months for CO [*Novelli et al.*, 1998], 2–3 months for C_2H_6 [*Blake and Rowland*, 1986; *Hough*, 1991], and 2–4 months for HCN [*Li et al.*, 2000]). Analysis of over 24,000 ten-day kinematic back trajectories in the tropical and subtropical western Pacific for August–October 1996 showed rapid transport of emission outflow from source regions to the middle and upper free troposphere by common deep convection followed by rapid west-to-east transport by high-speed winds (30 m s^{-1}) of the subtropical jet stream [*Fuelberg et al.*, 1999, Figure 4] near 30°S latitude. These high-altitude plumes of pollution travel thousands of kilometers in a few days and are not detected by surface in situ sampling measurements [e.g., *Novelli et al.*, 1998].

Biomass burning regularly occurs in tropical regions of Africa, South America, Australia, and Indonesia at the beginning of the dry season with timing that varies depending on the location [*Hao and Liu*, 1994]. Burning over southern Africa and South America is usually much greater than over Australia and Indonesia [*Board et al.*, 1999], though the magnitude of the burning in a region varies depending on the prevailing weather conditions and rainfall patterns, which control the availability of fuel. Fire statistics for 1997/1998 relative to 1996/1997 and 1993/1994 indicate relatively mild burning over Australia [*Olson et al.*, 1999, section 3.1] during the time period of our observations. Measurements during several aircraft campaigns [*Fishman et al.*, 1996; *Lindesay et al.*, 1996; *Hoell et al.*, 1999; *Blake et al.*, 1999] have documented the outflow of biomass burning pollutants and aerosols from southern hemisphere tropical regions during the dry season. Although these observations provide precise sampling and represent some of the few observations of middle and upper tropospheric chemistry in this remote region, mission duration was limited to a few weeks, and spatial coverage was sparse.

A multiyear time series of solar spectroscopic measurements of CO and C_2H_6 with maximum sensitivity in the upper troposphere has been reported from Lauder, New Zealand

Paper number 2000JD000318.
0148-0227/01/2000JD000318$09.00

(45.0°S, 169.7°E, 0.37 km altitude), for July 1993 to November 1997 [*Rinsland et al.*, 1998a]. An earlier set of C_2H_6 measurements from Lauder was also reported for December 1992 to March 1994 [*Rinsland et al.*, 1994]. Both sets of measurements show elevated columns each year above the station during the tropical dry season. High variability is observed near the austral spring maximum [e.g., *Rinsland et al.*, 1998a, Figure 10], as the Lauder station is sufficiently far south that tropical or clean midlatitude air are sampled alternately with sampling changes that occur irregularly on a timescale of several days [*Pougatchev et al.*, 1999].

Although in situ gas chromatographic measurements of CO, CH_4, and other trace gases have been obtained for several years from the station at Cape Grim, Tasmania (40.7°S, 144.7°E), [*Prinn et al.*, 2000; *Pak*, 2000], few free tropospheric measurements have been reported above Australia. Enhanced levels of CO, O_3, and other pollutants were measured over northern Australia near the tropopause during October 1994 [*Folkins et al.*, 1997], consistent with Measurement of Air Pollution From Satellites (MAPS) measurements during the same time period [*Connors et al.*, 1999]. A field campaign in austral spring of 1998 showed the presence of large horizontal layers of enhanced free tropospheric aerosols highly correlated with excess ozone over Mildura, Australia (34°S, 140°E) [*Rosen et al.*, 2000].

The infrared remote sensing measurements of CO, C_2H_6, and HCN reported here were recorded with the high spectral resolution Fourier transform spectrometer (FTS) at a complementary station of the Network for the Detection of Stratospheric Change (NDSC) [*Kurylo*, 1991; *Kurylo and Zander*, 2000, URL: http://www.ndsc.noaa.gov]. They represent a unique time series of solar absorption measurements for assessing the impact of tropical biomass burning emissions on tropospheric chemistry at southern midlatitudes. The measurements were recorded from the NDSC station with a FTS located closest to the southern hemisphere tropical biomass source regions. They are the first ground-based midlatitude southern hemisphere measurements of HCN, a sensitive indicator of biomass burning emissions [*Li et al.*, 2000] as demonstrated from shuttle-borne [*Rinsland et al.*, 1998b] and ground-based infrared spectroscopic measurements [*Rinsland et al.*, 1999, 2000, 2001; *Notholt et al.*, 2000; *Zhao et al.*, 2000a, 2000b].

The measurements reported here have maximum sensitivity in the upper troposphere and were recorded during one of the two most intense El Niño–Southern Oscillation (ENSO) events since 1970 [*Chandra et al.*, 1998; *Rinsland et al.*, 2001]. Intense and widespread wildfires occurred in the tropical Pacific rain forests of Sumatra and Borneo during 1997–1998 as a result of abnormal dryness in the region [e.g., *Liew et al.*, 1998; *Levine*, 1999]. Air samples at 8–13 km collected on board a commercial airliner during flights between Australia and Japan between April 1993 and December 1997 showed an anomalous CO increase during September to December 1997 in the southern hemisphere tropics [*Matsueda et al.*, 1999]. Peak CO mixing ratios of 320–380 ppbv (1 ppbv = 10^{-9} parts per unit volume) were measured during October 1997 at 20°S latitude. The elevated CO levels were first observed between 14°S–28°S during late October and disappeared in the beginning of December. We report back trajectory calculations performed for days with elevated CO, C_2H_6, and HCN tropospheric columns above the Wollongong station to determine the origin of the emissions.

2. Measurements and Analysis

The infrared solar absorption spectra were recorded with a Bomem model DA-8 Fourier transform spectrometer operated by the Atmospheric Chemistry Research Group of the University of Wollongong on the Australian east coast (34.45°S, 150.88°, 30 m asl). The station is located 56 km south of the main Sydney airport. While the site is usually free of local pollution, there are occasional episodes of elevated CO levels originating from traffic or local industry. The emissions influence only the lowermost atmospheric layers. Days with observed local CO pollution did not correlate with the CO, C_2H_6, and HCN time series reported here, which sample the atmosphere with high sensitivity in the upper troposphere and low sensitivity near the surface.

The Wollongong FTS is routinely operated with a maximum optical path difference of 250 cm corresponding to a maximum resolution of 0.004 cm^{-1} [*Griffith et al.*, 1998]. Spectra are recorded unapodized with either an InSb or a HcCdTe detector in combination with one of a set of optical filters that limit the band pass to intervals 650–1000 cm^{-1} wide. We focus here on measurements recorded with the InSb detector, which provided a higher signal-to-noise ratio. Observations with this instrument have been recorded from the University of Wollongong station since May 1996. The standard observing procedure is to coadd four interferograms requiring approximately 11 min for full resolution scans. Absolute accuracy of the measurement timings is better than 1 s.

Temperature profiles adopted for the analysis are based on pressure-temperature-geopotential altitude radiosondes launched from the main Sydney airport. A profile from a morning or evening radiosonde flight was spline-fitted into daily mean National Centers for Environmental Prediction (NCEP) profiles calculated for the location of the Wollongong station. The temperature profile was extended above the upper altitude limit of the NCEP measurements (~65 km) by smoothly connecting it to a climatological profile for the appropriate season of the observation. Further, daily water vapor volume mixing ratios were calculated from the relative humidity data provided by the radiosonde data and spline-fitted into a climatology above the tropopause.

Tropopause altitudes have been derived from the Sydney airport radiosondes. A fit to the measurements between January 1995 and December 1999 shows the average tropopause altitude varies with season from a maximum of 16 km in January to a minimum of 12 km in June. On this basis we adopted an annual mean tropopause height of 14 km for calculation of tropospheric columns from the present measurements. In this paper we use the term "tropospheric columns" to denote partial column abundances obtained in the 0.03–14 km altitude range, irrespective of the actual tropopause altitude on a particular day.

The Wollongong measurements have been analyzed with SFIT2, an algorithm developed at NASA Langley Research Center and the New Zealand National Institute of Water and Atmospheric Research (NIWA) (see *Pougatchev et al.* [1995] and *Rinsland et al.* [1998a] for an overview). Inversions are based on a semiempirical application [e.g., *Connor et al.*, 1995] of the optimal estimation formalism [*Rodgers*, 1990].

A priori volume mixing ratio profiles for CO, C_2H_6, and HCN were adopted from several sources. The covariance matrix for each target species was assumed to be diagonal with the uncertainties expressed relative to the a priori mixing ratio in

the layer. Relative uncertainties were set to 0.2 for CO, 0.2–0.5 for C_2H_6, and 0.5 for HCN in the 29 forward model layers, which extended from the surface to 100-km altitude. Signal-to-noise ratios of 200, 200, and 500 were adopted in the retrievals for CO, C_2H_6, and HCN, respectively. The strategy for the a priori profile and other parameter selections was to adjust them to achieve very similar vertical sampling of the troposphere based on averaging kernels while achieving excellent fits to the measured spectra. Vertical layer thickness in the forward model increases from less than 1 km in the first layer to 1 km below 10 km and 2 km for altitudes between 10 and 30 km. Higher-altitude layers are broader. Refractive ray tracing was performed with an improved version (A. Meier et al., manuscript in preparation, 2001) of FSCATM [*Gallery et al.*, 1983]. Air mass distributions, density-weighted temperatures, and density-weighted pressures were calculated for each layer.

The tropospheric portion of the CO a priori profile was computed from the mean of April and October profiles measured over Bass Strait and Cape Grim, Tasmania. Both profiles [*Pougatchev et al.*, 1998, Figure 3] peak in the upper troposphere with higher mixing ratios measured during October than April. The average profile was smoothly connected to a distribution with a minimum of 10 ppbv at 25-km altitude increasing above due to CO production from CO_2 photolysis. The assumed a priori CO profile is consistent with the measurements reported by *Pak* [2000].

The tropospheric C_2H_6 a priori profile is an average of March, June, and December profiles computed for the latitude of Wollongong with a global two-dimensional model [*Kanakidou et al.*, 1991, Figure 7]. The mean profile also peaks in the upper troposphere. An exponential decrease with a 3-km scale height was assumed above the tropopause [*Rinsland et al.*, 1987].

Retrievals of HCN were performed with two different a priori profiles. The first, which we refer to as the "standard" profile, assumes a distribution with a peak of 190 pptv (10^{-12} per unit volume) at the surface, decreasing to mixing ratios of 180 pptv at 12 km and 155 pptv at 30 km. This distribution is similar to those adopted in previous studies [*Rinsland et al.*, 1998, 1999, 2000, 2001]. It is based on model calculations which predict a 5% mixing ratio decrease between 0 and 12 km with a more rapid decline in the stratosphere due to HCN reaction with OH and $O(^1D)$ [*Cicerone and Zellner*, 1983, Figure 3]. The model-predicted lifetime of 2.5 years is significantly longer than the recent 3-D model estimate of 2–4 months that assumes an ocean sink for HCN to account for the observed variability in the troposphere [*Li et al.*, 2000]. The second HCN a priori profile, referred to as the "model2000" profile, assumes the annual mean, zonal-average profile calculated for the latitude of Wollongong [*Li et al.*, 2000, Figure 2]. This distribution increases from 120 pptv at the surface to a broad maximum of 220 pptv in the upper troposphere with a decline above. A decrease at higher altitudes is due to HCN reaction with OH and $O(^1D)$.

Microwindows and interfering molecules are listed in Table 1. The two windows adopted for the CO analysis and the single window for the C_2H_6 retrievals are the same ones as used in a previous study of solar spectra recorded from several stations [*Rinsland et al.*, 1998a, 1999].

The retrieval of HCN was more difficult than in our previous studies due to the very high water vapor columns above the Wollongong site as compared to those above high-altitude stations as a result of both the low elevation (30 m) and the humid coastal location. Low signal to noise in the HCN region has been reported for measurements from other low-altitude stations [*Zhao et al.*, 2000a]. We compensated for the lower signal to noise achievable from the Wollongong observations by adding two additional HCN microwindows to the microwindow for the P(8) ν_1 band line at 3287.25 cm^{-1}. To our knowledge, the microwindow for the P(14) HCN line at 3268.2229 cm^{-1} has not been used in previous ground-based studies. Molecule-by-molecule simulations of the transmission in this microwindow are available from the authors as a yet unpublished update to an atlas of infrared microwindows [*Meier et al.*, 1997].

Table 1. Microwindows and Interferences[a]

Target Molecule	Microwindows, cm^{-1}	Interfering Molecules
CO	4274.62–4274.82, 4284.75–4285.18	solar CO, CH_4, HDO
C_2H_6	2976.65–2976.92	H_2O, CH_4, O_3
HCN	3268.18–3268.27	H_2O
	3287.15–3287.35	
	3299.46–3299.58	

[a]Notes: Each target molecule was fitted for profile retrieval. The profile of CH_4 was also retrieved from the fittings of the two CO windows at 4274.62–4274.82, 4284.75–4285.18. Interfering molecules were fitted by multiplicative scalings of the a priori volume mixing ratio profile by a single value. Isotopic $H_2{}^{17}O$ and $H_2{}^{18}O$ were fitted separately in the HCN analysis. Spectra with astronomical zenith angles above 85° were excluded.

Spectroscopic parameters for the CO, C_2H_6, and HCN target lines were the same as reported previously [*Rinsland et al.*, 1998a, 1999, 2000, 2001]. Parameters for the two additional HCN ν_1 band windows were adopted from HITRAN 1996 [*Rothman et al.*, 1998] to achieve consistency in the retrievals from the three microwindows. Recently reported (2-0) band room temperature measurements of CO-N_2 widths and shifts [*Predoi-Cross et al.*, 2000] and CO-O_2 and CO-N_2 (2-0) band room temperature pressure shifts [*Bouanich et al.*, 1996] were not considered to maintain consistency with respect to the previous analyses.

The standard deviation of the residuals was plotted against the depth of target line in each of the measured spectra. These two parameters were used to select criteria to identify noisy observations and measurements of weak absorption by the target spectral line. Such observations were deleted from the database [*Rinsland et al.*, 1998a, section 5].

3. Error Analysis

Table 2 presents estimates of the effects of random and systematic sources of error on the retrieved tropospheric columns. The analysis followed procedures adopted in previous studies [*Rinsland et al.*, 1998a, 1999, 2000, 2001] with each parameter offset by its 1-sigma uncertainty for one or more typical cases to quantify the errors.

Sources of random errors considered are the uncertainty in the assumed temperature profile, errors in the effective solar zenith angles of the individual spectra, and random instrumental noise. Profiles from the Sydney airport and NCEP temperatures were offset by 2 K in all atmospheric layers. This offset is larger than the quoted sonde errors in the troposphere, but it is less than the NCEP temperature uncertainties in the upper stratosphere. The calculated tropospheric CO, C_2H_6, and

Table 2. CO, C_2H_6, and HCN Tropospheric Column Measurement Uncertainties

Error Source	Relative Error, %		
	CO	C_2H_6	HCN
	Random Error Budget		
Temperature	0.5	0.2	1.3
Instrument noise[a]	0.7	1.2	1.5
Zenith angle	<1	<1	<1
Interfering lines	<1	<1	<1
RSS total random error	0.9	1.2	2.0
	Systematic Error Budget		
Spectroscopic parameters	2	5	5
A priori profile	6.1	20.4	40.7
Forward model approximations[b]	4	2	2
Instrument line shape function	0.1	0.2	<0.1
Zero level offsets	0.9	0.4	0.7
RSS total systematic error	7.6	21.1	41.0

[a]Based on the typical standard deviation of spectra satisfying the objective criteria for valid fits.
[b]Includes the uncertainty in the retrieval due to errors in computing the absorption by overlapping solar CO lines.

HCN column changed by <1% with respect to the unperturbed values. Errors in the effective solar zenith angles of the spectra are negligibly small as discussed in section 2. The largest source of random error was instrumental noise, particularly for CO and HCN. These errors are reduced significantly by averaging of the retrievals from multiple spectra on a day. The number of measurements per day satisfying the objective selection criteria ranged from 1–6 for CO, 1–11 for C_2H_6, and 1–5 for retrievals with both the HCN "standard" and "model2000" a priori profiles.

Sources of systematic error considered in the analysis were uncertainties in the spectroscopic parameters, the relative contribution of the a priori profile to the retrieval, forward model approximations, errors in modeling the instrument line shape (ILS) function, and zero level offsets in the spectra. The most important sources of systematic error are attributed to inaccuracies in the simulation of solar CO lines in the forward model, potential bias from the a priori profile (particularly for HCN), and possible errors in the HCN air-broadening coefficients (see *Rinsland et al.* [2000, section 4.5] for a discussion). Total estimated root-sum-square (RMS) random and systematic errors are 1 and 8% for CO, 1 and 21% for C_2H_6, and 2 and 41% for HCN, respectively. The relatively large systematic tropospheric column uncertainties can be attributed to the limited sensitivity of the CO, C_2H_6, and HCN measurements in the lower troposphere. However, sensitivity is good in the upper troposphere, the primary focus of this investigation.

4. Results and Discussion

Figure 1 presents the tropospheric column averaging kernels for CO, C_2H_6, and HCN profile retrievals based on the micro-

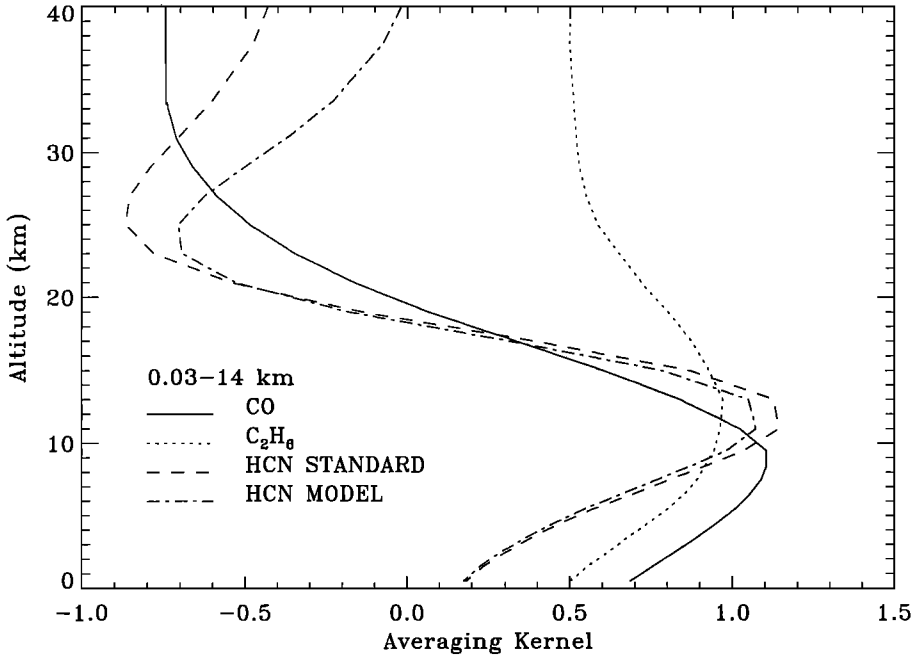

Figure 1. Averaging kernels calculated for CO, C_2H_6, and HCN profile retrievals. Values are shown for merged layers extending from 0.03–14 km altitude.

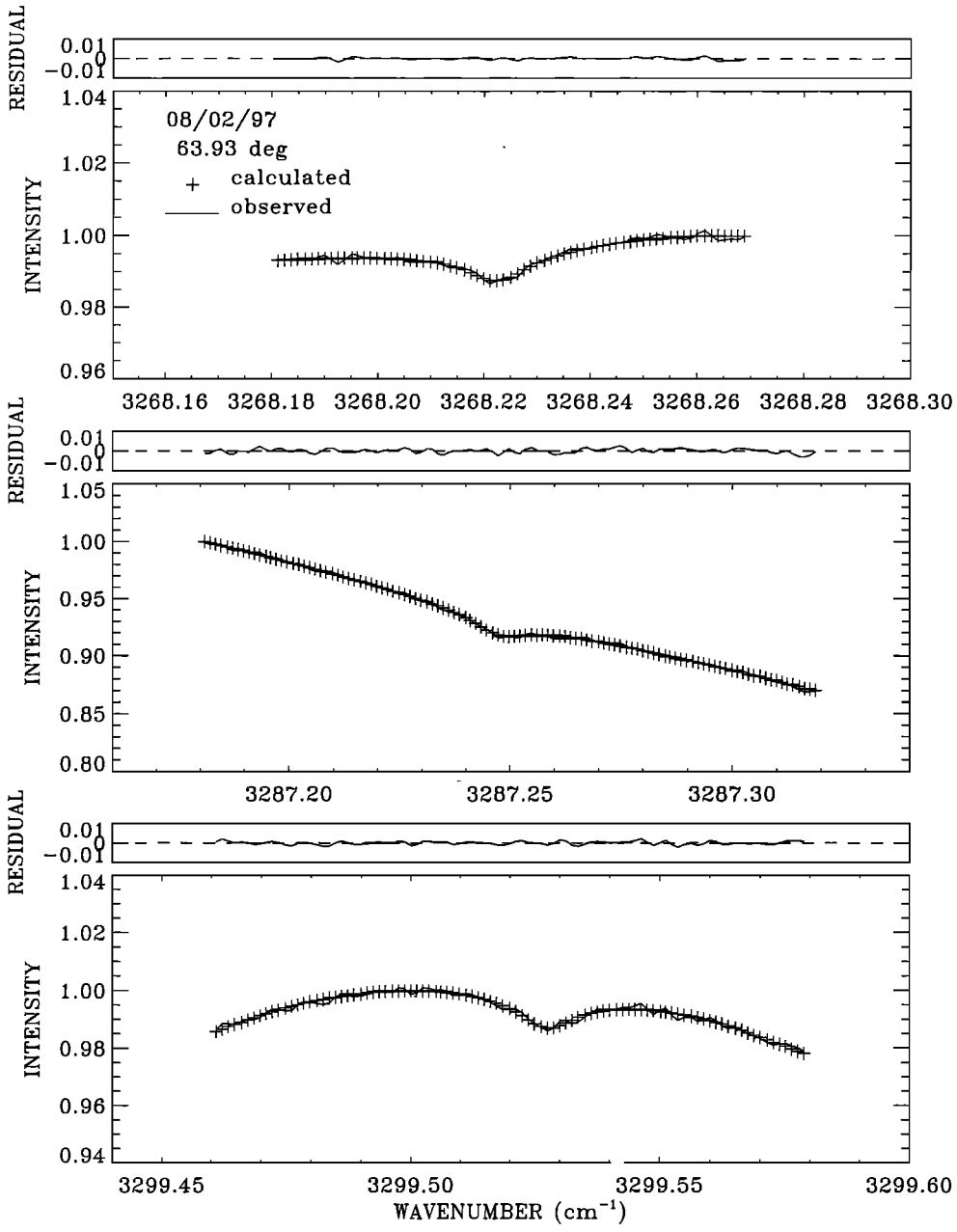

Figure 2. Sample spectral fit for the three HCN microwindows. The solar spectrum is displayed normalized to the peak value in each interval. The astronomical zenith angle and date of observation date are identified. Residuals (measured minus calculated values) are displayed above each fit.

windows and parameters described in section 2. The maximum sensitivity occurs at altitudes of 9.0 and 12.5 km for CO and C_2H_6, and at 11.9 and 11.8 km for the "standard" and "model2000" HCN a priori profiles, respectively.

Figure 2 presents a sample spectrum and fit for HCN to illustrate the consistency of the simultaneous analysis with the three HCN microwindows. The measured spectrum was analyzed assuming the standard HCN a priori profile. The spectral fit achieved with the model2000 profile is nearly identical. Although a previous study [*Mahieu et al.*, 1995] suggested a bias between total columns retrieved from the P(4) and P(8) ν_1 band lines, we found the windows and retrieval parameter selections yielded residuals from the simultaneous microwindow fits with no discernible bias in the residuals to the simultaneous fits to the three lines. Retrievals for CO and C_2H_6 are similar to those shown previously [e.g., *Rinsland et al.*, 1999, Figures 2 and 4].

Figure 3 presents the time series of daily average CO, C_2H_6, and HCN tropospheric columns retrieved from the Wollongong observations. Open circles show retrievals obtained for CO, C_2H_6, and the standard HCN a priori profile. Triangles in the bottom panel show HCN retrievals obtained with the model2000 a priori profile.

The daily average tropospheric columns C_t have been fitted with the expression

$$C_t = a_0 + a_1(t - t_0) + a_2 \cos 2\pi[(t - t_0) - \varphi], \quad (1)$$

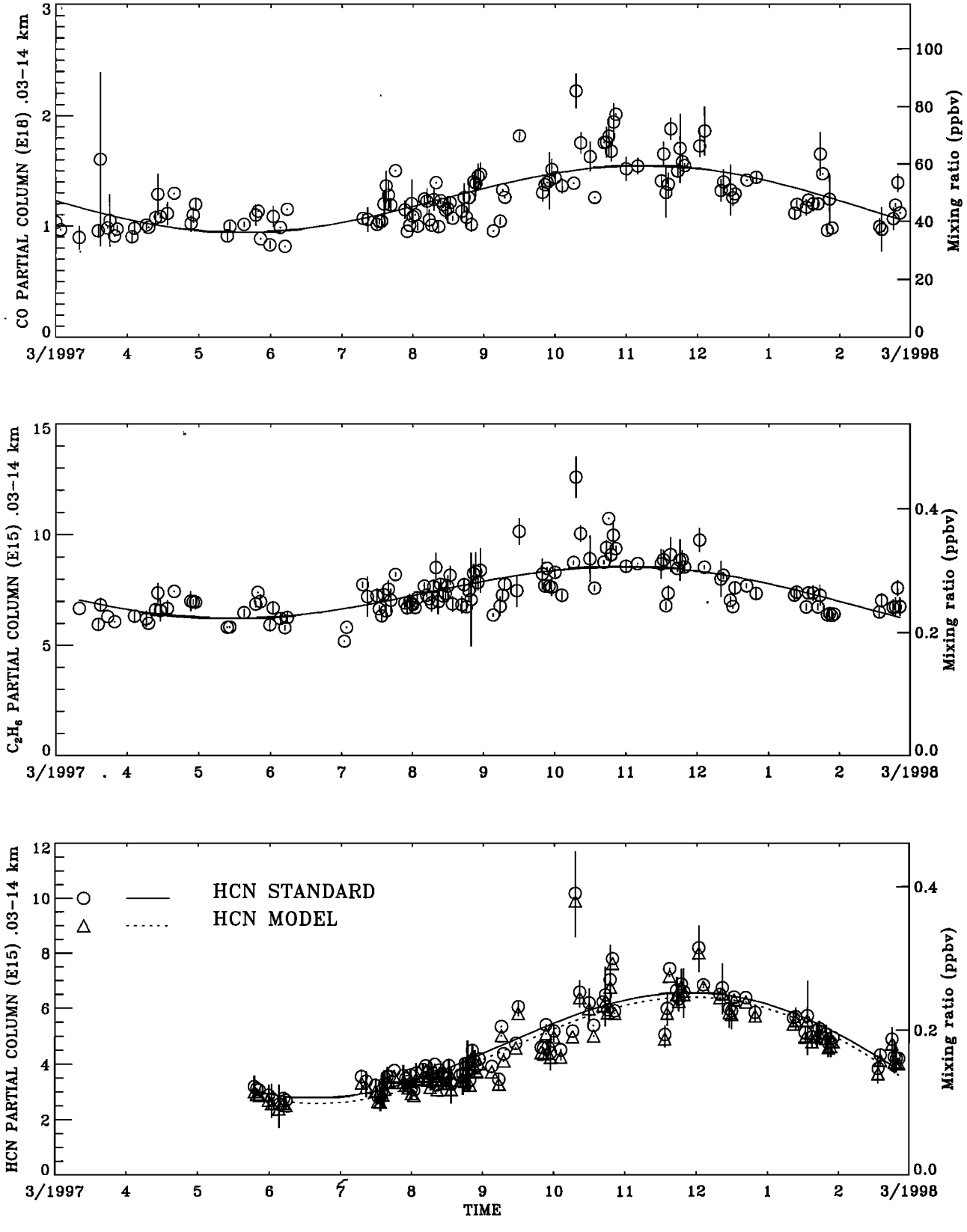

Figure 3. Time series of daily average tropospheric columns retrieved for CO, C_2H_6, and HCN from the Wollongong time series. Open circles with error bars represent the daily mean and standard deviation, respectively. Solid curves or dashed curves display fits to the daily averages with equation (1). Approximate average volume mixing ratios are illustrated on the right vertical axis.

Table 3. Coefficients From Fits to the Daily Average CO, C_2H_6, and HCN Tropospheric Column Time Series With Equation (1)[a]

Parameter	CO	C_2H_6	HCN (std)	HCN (Model)
a_0	1.14676	7.86999	5.57461	5.44507
a_1	0.115085 (0.0670395)	−1.17170 (0.471889)	−3.11448 (0.909031)	−3.25812 (0.897592)
a_2	0.254748 (0.0286513)	1.45266 (0.151801)	2.62039 (0.198606)	2.66753 (0.195928)
φ	−0.184444 (0.0159272)	0.156611 (0.0151704)	0.539815 (0.713025)	0.542664 (0.712666)
t_0	1997.0220	1997.1940	1997.3992	1997.3992
N/n	392/144	617/129	262/104	262/104

[a]Units for a_0, a_1, and a_2 are 0.03–14 km columns in 10^{15} molecules cm^{-2} for C_2H_6 and HCN and 10^{18} molecules cm^{-2} for CO. Parentheses show 1-sigma uncertainties. The total number N of valid measurements and the number of days n with one or more valid measurements are reported. The coefficients labeled "std" and "model" refer to results obtained with the "standard" and "model2000" a priori profiles.

where a_0 is the mean value, t is the observation time in calendar years, t_0 is the time of the first observation in calendar years, a_1 is the long-term trend, a_2 is the amplitude of the seasonal cycle (assumed to be sinusoidal), and φ is the fraction of the calendar year corresponding to the seasonal cycle maximum. The best fits to the daily averages are shown in Figure 3 with solid curves except for the fit to the HCN daily averages retrieved with the model2000 a priori profile, which is illustrated with a dashed curve. The ratio and standard deviation of the model2000 to the standard daily average tropospheric profiles are 0.95 and 0.02, respectively. Hence there is only a small difference between the two sets of tropospheric columns.

The coefficients obtained with (1) are reported in Table 3. The trends are not reliable due to the short time period of the measurements. All three molecules show distinct seasonal variations with maximum tropospheric columns and upper tropospheric mixing ratios during austral spring and a minimum during austral autumn. Unfortunately, observations with the optical filter most suitable for measuring HCN did not begin until May 1997, though the quality of the observations after that time was quite good despite the low altitude of the station. As shown in the plot, HCN variations exceeded those of CO and C_2H_6 with best fit maximum and minimum tropospheric HCN columns of 6.56 and 2.78 (in 10^{15} molecules cm^{-2}) retrieved with the standard a priori profile, respectively.

Figure 4 displays HCN volume mixing ratio versus altitude profiles retrieved with the standard and model2000 a priori profiles for the February–July (top) and August–December (bottom) time periods. Although emissions from biomass burning vary considerably by location and from year to year, the selected time periods correspond roughly to background and biomass-enhanced time periods in the southern hemisphere tropical Africa and South America. Solid circles with error bars represent the mean and standard deviation of the profiles, respectively. Average profiles for the two time periods show striking differences. The dry season profiles (bottom panel) show maximum average mixing ratios of 0.4 ppbv at 11 km altitude as compared to mixing ratio of 0.2 ppbv or less for the background time period (top panels). The agreement between the retrieved profiles in the upper troposphere is consistent with the good sensitivity indicated by the averaging kernels in Figure 1. The reduced sensitivity of the measurements near the surface can be noted by comparing the retrievals with the a priori profiles at low altitudes. The retrievals are close to the corresponding standard or model2000 a priori profiles. Hence we conclude the Wollongong retrievals have insufficient sensitivity in the lower troposphere to confirm or disprove the HCN ocean sink hypothesis [*Li et al.*, 2000].

Our measurements with their good sensitivity in the upper troposphere provide further evidence for the importance of HCN in that region. Upper troposphere total reactive nitrogen (NO_y) levels calculated by summing the mixing ratios of individual components during recent airborne Global Tropospheric Experiment (GTE) field missions (HNO_3 + NO + NO_2 + PAN) are on average slightly less than half the mixing ratio measured by an NO_y detector on board the same aircraft [*Bradshaw et al.*, 1998]. The "missing" NO_y is likely to result primarily from HCN surface emissions from fires lofted by deep convection and transported long-distances, but unmeasured by the GTE instrumentation used at the time [*Smyth et al.*, 1996; *Rinsland et al.*, 1999; *Li et al.*, 2000].

Figure 5 presents a plot of the tropospheric daily average C_2H_6 column versus the daily average tropospheric CO column. The dashed line indicates a best fit to the measurements. The correlation coefficient is 0.88, suggesting a very similar lifetime for both molecules with a common source for their emissions, namely, tropical biomass burning emissions from southern hemisphere source regions. A tight positive correlation between CO and C_2H_6 tropospheric columns has been reported previously from ground-based solar absorption spectra recorded from stations in both hemispheres [*Rinsland et al.*, 1998a, 1999, Table 6 and Figure 5, 2000, Figure 6]. In situ aircraft measurements also show a tight correlation between CO and C_2H_6 tropospheric mixing ratios [e.g., *Blake et al.*, 1996, Figure 3, 1999, Figures 2 and 6]. The ground-based spectroscopic data sets show the C_2H_6/CO slope is higher at northern hemisphere middle to high latitudes than in the southern hemisphere.

The positive correlation of tropospheric HCN with CO in both hemispheres has been cited as evidence for a dominant HCN biomass burning source [*Li et al.*, 2000]. Figure 6 presents the correlation between the HCN and CO tropospheric columns from the Wollongong time series. The retrievals were obtained with the standard HCN a priori profile and daily average February–July (top) and August–December (bottom) measurements displayed separately, consistent with our selections of these periods as characteristic background and tropical biomass burning seasons, respectively. The tropospheric columns from the biomass burning time period show a wider range of variations, a higher HCN/CO slope, and a more compact correlation relative to the corresponding measurements from the background time period. The slope of the HCN/CO tropospheric columns ratio is well within the range of previous ground-based tropospheric column measurements [*Rinsland et al.*, 1999] and field emission measurements of 0.0049–0.0581 [*Lobert et al.*, 1991]. Correlation coefficients of HCN and CO from 0.34 to 0.95 have been derived from other ground-based observation sets [*Rinsland et al.*, 1999, 2000; *Zhao et al.*, 2000a].

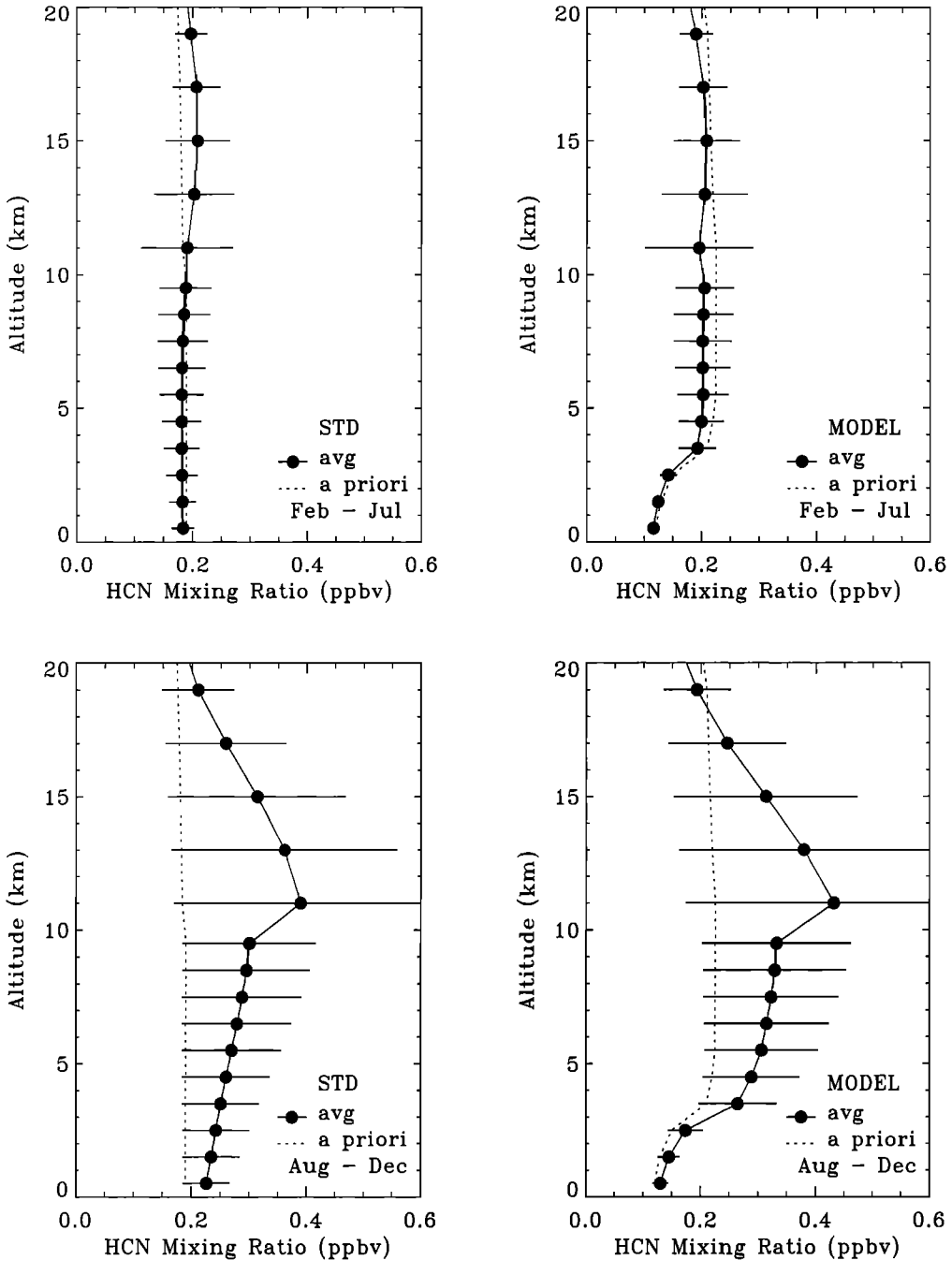

Figure 4. HCN vertical profiles retrieved for (top) background and (bottom) biomass burning enhanced time periods in tropical Africa and South America. Dashed lines identify the "standard" or "model2000" a priori profiles (see text). Average profiles are shown with solid circles. Horizontal error bars represent the standard deviation of the daily mean mixing ratios measured in each forward model layer.

The highest correlation coefficient and highest HCN/CO tropospheric columns slope were measured above Mauna Loa in air that recently originated from the intense tropical Asian fires of 1997–1998 [*Rinsland et al.*, 1999]. The Wollongong HCN/CO columns ratio for the biomass burning period is lower than the ratio from those measurements by a factor of 2. The lower correlation coefficients between HCN and CO typically measured above northern hemisphere sites are due to the significant contributions of urban and industrial emissions to the CO tropospheric budget.

The Wollongong infrared spectra contain spectral regions suitable for detection of spectral features of shorter-lived biomass burning products such as C_2H_2 with losses determined by a combination of OH photochemistry and turbulent mixing during transport [e.g., *McKeen et al.*, 1996; *Smyth et al.*, 1999]. In general, these processes cannot be distinguished. Absorption by the C_2H_2 $\nu_2 + \nu_4 + \nu_5$ band P13 line at 3250.6633 cm^{-1} was near or below the detection limit in the Wollongong spectra. Simulations for a solar zenith angle of 80° were performed assuming the spectroscopic parameters from the HITRAN

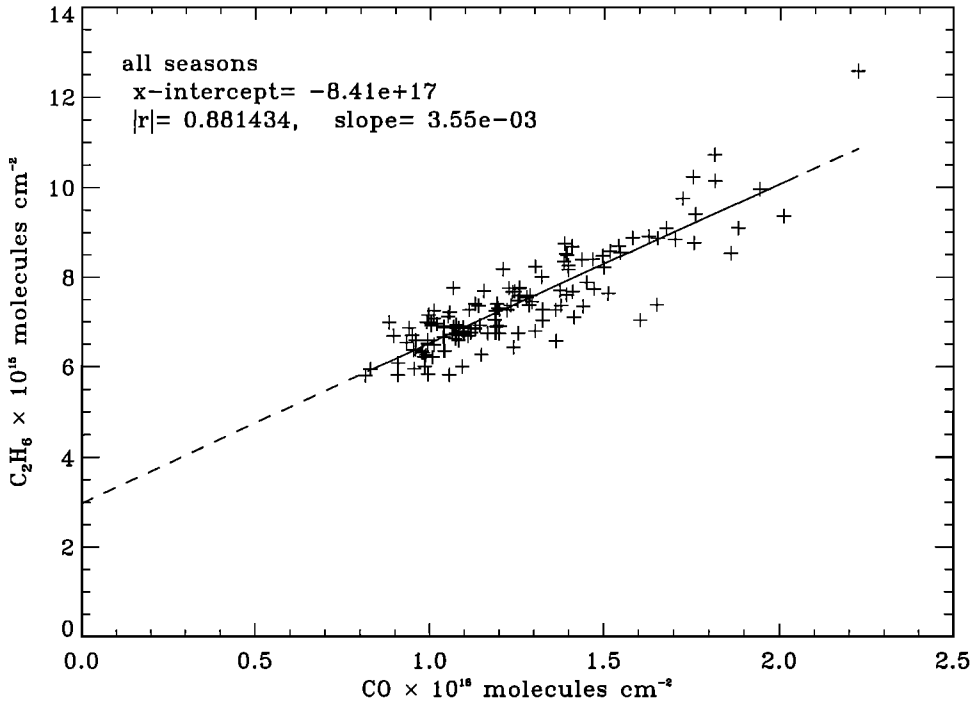

Figure 5. CO versus C_2H_6 tropospheric columns from the Wollongong time series. Measurements from all seasons are included. The dashed line shows the best fit slope derived from an unweighted fit to the column measurements. The correlation coefficient is also reported.

1996 compilation [*Rothman et al.*, 1998] with a constant mixing ratio assumed in the troposphere and zero above. The simulations indicate a tropospheric upper limit of 200 pptv, consistent with observations of no local biomass burning events on any solar observation days and the absence of this C_2H_2 absorption feature in the solar spectra.

5. Back Trajectory Calculations and Their Implications

Figure 7 illustrates 7-day isentropic back trajectories computed beginning at the 340 K potential temperature θ (~11 km altitude) level above Wollongong on selected days between October and December 1997 obtained with the NASA Goddard automailer. The selected θ level is close to the maximum sensitivity of the CO, C_2H_6, and HCN tropospheric column averaging kernels, as illustrated in Figure 1. The trajectory analyses assume meteorological fields from the National Centers for Environmental Prediction (NCEP) analyses with balance equation computed winds. If the NCEP analyses were not available, forecast fields were used according to the recommended documentation for the trajectory model [*Schoeberl and Sparling*, 1994] and the Goddard Assimilation data [*Takacs et al.*, 1994]. Although individual trajectories are uncertain for a variety of reasons [*Merrill*, 1996], especially after several days in remote regions, our results for an ensemble of cases suggest the measured elevated upper tropospheric columns originated from near-zonal west-to-east transport. Most trajectories passed over southwest Australia after crossing land over southern Africa and/or South America, where already noted, the most intense fires normally burn during this time period. The photochemical lifetimes of CO, C_2H_6, and HCN are sufficiently long for air parcels to traverse the globe multiple times with minor losses. The upper tropospheric trajectories in Fig-

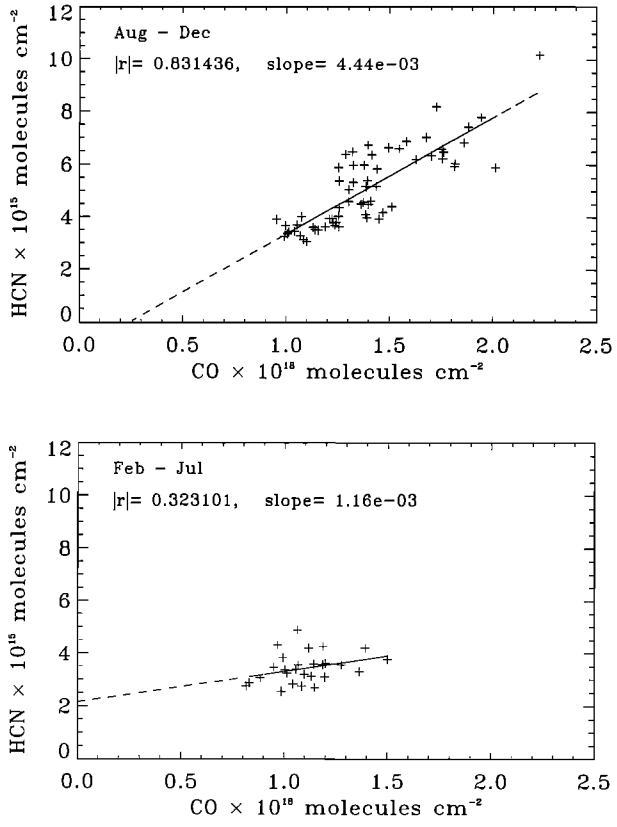

Figure 6. Daily average CO versus HCN tropospheric columns (pluses) for (top) background and (bottom) biomass burning enhanced time periods in tropical Africa and South America. The retrievals were performed with the "standard" HCN a priori profile.

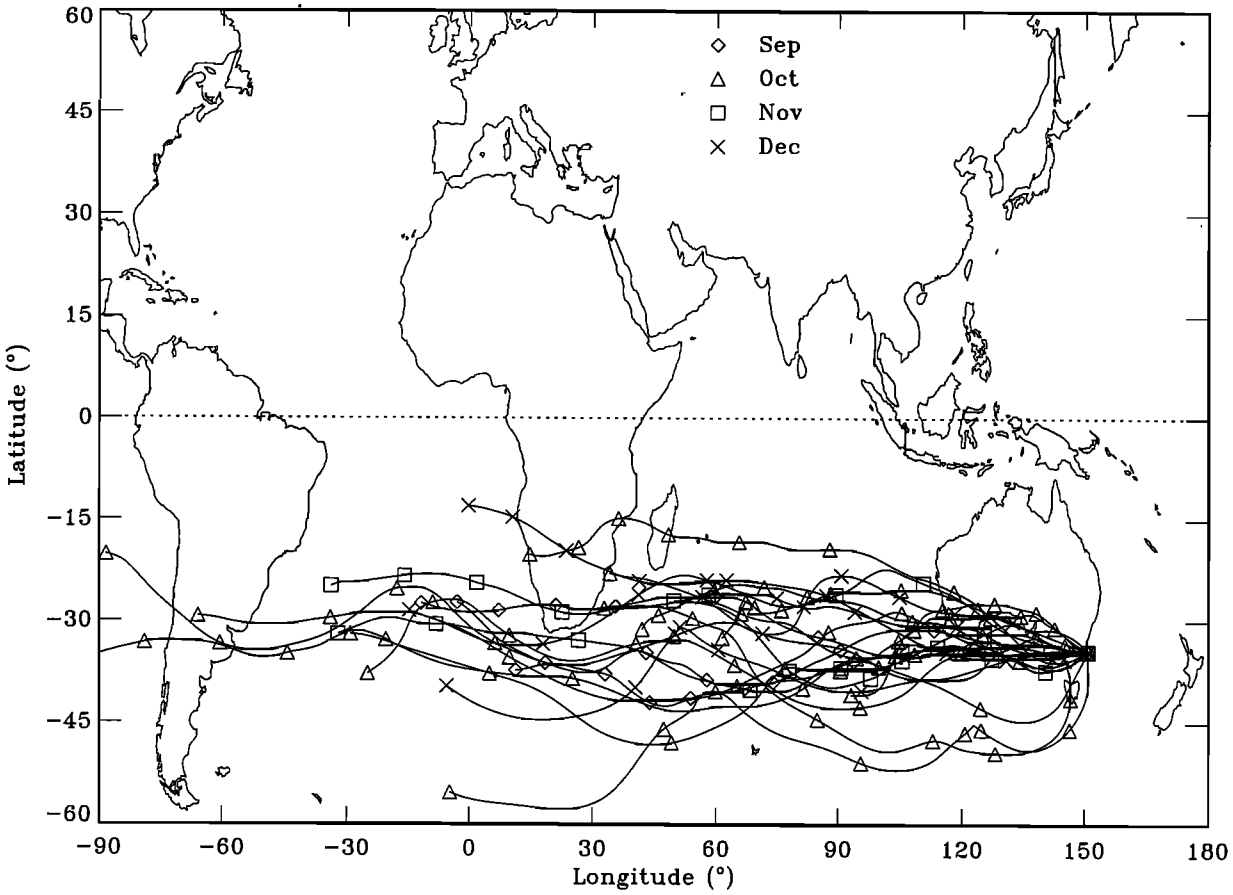

Figure 7. Seven-day back trajectories computed beginning at the 360 K potential temperature level for sample Wollongong measurements obtained during the October–December 1997 time period when the highest tropospheric CO, C_2H_6, and HCN columns were measured. Symbols represent 1-day time intervals along the trajectory path. A short-dashed line shows the equator.

ure 7 passed significantly south of the western Pacific equatorial regions where intense fires [*Chandra et al.*, 1998; *Liew et al.*, 1998; *Levine*, 1999] burned during October–December 1997 and CO upper tropospheric mixing ratios as high as 380 ppbv were measured [*Matsueda et al.*, 1999]. Hence we conclude the intense western Pacific tropical fires from the strong El Niño of 1997–1998 had no significant impact on the Wollongong observations.

6. Summary and Conclusions

We have analyzed a time series of 0.004-cm^{-1} resolution infrared solar absorption spectra recorded over 100 days between March 1997 to February 1998 at the Network for the Detection of Stratospheric Change complementary station at the University of Wollongong, Australia (34.45°S, 150.88°E, 30 m asl). Retrievals of CO, C_2H_6, and HCN were performed with the SFIT2 algorithm with microwindows selected to achieve maximum sensitivity in the upper troposphere. The time series show a seasonal maximum for all three molecules during October–December 1997 with best fit peak tropospheric columns of 1.54×10^{18}, 8.56×10^{15}, and 6.56×10^{15} molecules cm^{-2}, respectively. The period of high columns corresponds with the dry season in the southern hemisphere tropics. Tropospheric CO and C_2H_6 columns were highly correlated throughout the year with a C_2H_6/CO slope of 0.00355 close to that measured above Lauder, New Zealand (45.0°S, 169.7°E, 0.37 km altitude), of 0.00338–0.00504. Both values are much lower than measured from northern hemisphere sites, for example, 0.0142 from Kitt Peak at 31.9°N latitude [*Rinsland et al.*, 1998b]. The HCN and CO tropospheric columns also show a positive correlation with a higher slope and more compact relation during the burning season than during the background time period. Seven-day isentropic back trajectory calculations performed for upper tropospheric levels on selected observation days during the October–December maximum show rapid west-to-east near-zonal transport over transcontinental distances often passing over Africa and/or South America. On this basis we conclude the elevated tropospheric columns measured during this time period likely originated primarily from active biomass burning regions in these continents, where the most intense fires are typically observed during austral spring. Although geographically closer, the back trajectories did not pass close to the more northerly New Guinea-Borneo-Indonesia tropical region. Hence we conclude the elevated CO, C_2H_6, and HCN tropospheric columns observed above Wollongong were not significantly impacted by the intense El Niño–related tropical Asian emissions from the same time period. This conclusion is consistent with in situ aircraft measurements of a sharp decline in CO upper tropospheric mixing ratio between 20°S and 30°S latitude and nearly

the same longitude during this time period [*Matsueda et al.*, 1999, Figure 2 and Plate 1]. The absence of C_2H_2 absorptions above the noise level on days with elevated CO, C_2H_6, and HCN tropospheric columns confirms observations that indicate local fires were not the source of the pollution. Analysis of Wollongong spectra from other time periods is planned to quantify interannual variations and provide measurements of additional species.

Acknowledgments. Research at NASA Langley Research Center was funded by NASA's Upper Atmosphere Research and the Atmospheric Chemistry Modeling and Analysis Programs. We thank Fred Turatti, Stephen Wilson, Cirilo Bernardo, Frances Phillips, and Ian Jamie who helped record the solar spectra. We also thank the Atmosphere Watch Section of the Australian Bureau of Meteorology for access to their radiosonde measurements and NASA Goddard Space Flight Center for access and help with the use of the automailer trajectory program.

References

Blake, D. R., and F. S. Rowland, Global atmospheric concentrations and source strength of ethane, *Nature*, *321*, 231–233, 1986.

Blake, N. J., D. R. Blake, B. C. Sive, T.-Y. Chen, F. S. Rowland, J. E. Collins, G. W. Sachse, and B. E. Anderson, Biomass burning emissions and vertical distribution of atmospheric methyl halides and other reduced carbon gases in the South Atlantic region, *J. Geophys. Res.*, *101*, 24,151–24,164, 1996.

Blake, N. J., et al., Aircraft measurements of the latitudinal, vertical, and seasonal variations of NMHCs, methyl nitrate, methyl halides, and DMS during the First Aerosol Characterization Experiment (ACE 1), *J. Geophys. Res.*, *104*, 21,803–21,817, 1999.

Board, A. S., H. E. Fuelberg, G. L. Gregory, B. G. Heikes, M. G. Schultz, D. R. Blake, J. E. Dibb, S. T. Sandholm, and R. W. Talbot, Chemical characteristics of air from different source regions during the Pacific Exploratory Mission-Tropics A (PEM-Tropics A), *J. Geophys. Res.*, *104*, 16,181–16,196, 1999.

Bouanich, J.-P., D. Bermejo, J. L. Domenech, R. Z. Martinez, and J. Santos, Pressure-induced lineshifts in the 2 ← 0 band of CO self-perturbed and perturbed by He, Kr, O_2, and N_2, *J. Mol. Spectrosc.*, *179*, 22–31, 1996.

Bradshaw, S., S. T. Sandholm, and R. Talbot, An update on reactive odd-nitrogen measurements made during recent NASA Global Tropospheric Experiment programs, *J. Geophys. Res.*, *103*, 19,129–19,148, 1998.

Chandra, S., J. R. Ziemke, W. Min, and W. G. Read, Effects of 1997–1998 El Niño on tropospheric ozone and water vapor, *Geophys. Res. Lett.*, *25*, 3867–3870, 1998.

Cicerone, R. J., and R. Zellner, The atmospheric chemistry of hydrogen cyanide (HCN), *J. Geophys. Res.*, *88*, 10,689–10,696, 1983.

Connor, B. J., A. Parrish, J.-J. Tsou, and M. P. McCormick, Error analysis for the ground-based microwave ozone measurements during STOIC, *J. Geophys. Res.*, *100*, 9283–9291, 1995.

Connors, V. S., B. B. Gormsen, S. Nolf, and H. G. Reichle Jr., Spaceborne observations of the global distribution of carbon monoxide in the middle troposphere during April and October 1994, *J. Geophys. Res.*, *104*, 21,455–21,470, 1999.

Fishman, J., K. Fakhruzzaman, B. Cros, and D. Nganga, Identification of widespread pollution in the southern hemisphere deduced from satellite analyses, *Science*, *252*, 1693–1696, 1991.

Fishman, J., J. M. Hoell, R. D. Bendura, R. J. McNeal, and V. W. J. H. Kirchoff, NASA GTE GTE TRACE-A experiment (September–October 1992): Overview, *J. Geophys. Res.*, *101*, 23,865–23,880, 1996.

Folkins, I., R. Chatfield, D. Baumgardner, and M. Proffitt, Biomass burning and deep convection in southeastern Asia: Results from ASHOE/MAESA, *J. Geophys. Res.*, *102*, 13,291–13,299, 1997.

Fuelberg, H. E., R. E. Newell, S. P. Longmore, Y. Zhu, D. J. Westberg, E. V. Browell, D. R. Blake, G. L. Gregory, and G. W. Sachse, A meteorological overview of the Pacific Exploratory Mission (PEM) Tropics period, *J. Geophys. Res.*, *104*, 5585–5622, 1999.

Gallery, W. O., F. X. Kneizys, and S. A. Clough, Air mass computer program for atmospheric transmittance/radiance calculation: FSCATM, *Environ. Res. Pap. 828 (AFGL-TR-83-0065)*, 145 pp., Air Force Geophys. Lab., Bedford, Mass., 1983.

Griffith, D. W. T., N. B. Jones, and W. A. Mathews, Interhemispheric ratio and annual cycle of carbonyl sulfide (OCS) total column from ground-based solar FTIR spectra, *J. Geophys. Res.*, *103*, 8447–8454, 1998.

Hao, W. M., and M.-H. Liu, Spatial and temporal distribution of tropical biomass burning, *Global Biogeochem. Cycles*, *8*, 495–503, 1994.

Hoell, J. M., D. D. Davis, D. J. Jacob, M. O. Rodgers, R. E. Newell, H. E. Fuelberg, R. J. McNeal, J. L. Raper, and R. J. Bendura, Pacific Exploratory Mission in the tropical Pacific: PEM-Tropics A, August–September 1996, *J. Geophys. Res.*, *104*, 5567–5583, 1999.

Hough, A. M., Development of a two-dimensional global tropospheric model: Model chemistry, *J. Geophys. Res.*, *96*, 7325–7362, 1991.

Kanakidou, M., H. B. Singh, K. M. Valentin, and P. J. Crutzen, A two-dimensional study of ethane and propane oxidation in the troposphere, *J. Geophys. Res.*, *96*, 15,395–15,413, 1991.

Kurylo, M. J., Network for the detection of stratospheric change, *Proc. Soc. Photo Opt. Instrum. Eng.*, *1491*, 169–174, 1991.

Kurylo, M. J., and R. J. Zander, The NDSC—Its status after 10 years of operation, in *Proceedings of XVIV Quadrennial Ozone Symposium*, Hokkaido Univ., Sapporo, Japan, 2000.

Levine, J. S., The 1997 fires in Kalimantan and Sumatra, Indonesia, *Geophys. Res. Lett.*, *26*, 815–818, 1999.

Li, Q., D. Jacob, I. Bey, R. M. Yantosca, Y. Zhao, Y. Kondo, and J. Notholt, Atmospheric hydrogen cyanide: Biomass burning source, ocean sink? *Geophys. Res. Lett.*, *27*, 357–360, 2000.

Liew, S. C., O. K. Lim, L. K. Kwoh, and H. Lim, A study of the 1997 fires in South East Asia using SPOT quicklook mosaics, paper presented at the 1998 International Geoscience and Remote Sensing Symposium, Inst. of Electr. and Electr. Eng., Seattle, Wash., July 6–10, 1998.

Lindesay, J. A., M. O. Andreae, J. G. Goldammer, G. Harris, H. J. Annegarn, M. Garstang, R. J. Scholes, and B. W. van Wilgen, International Geosphere-Biosphere Programme/International Global Chemistry SAFARI-92 field experiment: Background and overview, *J. Geophys. Res.*, *101*, 23,521–23,530, 1996.

Lobert, J. M., D. H. Scharffe, W.-M. Hao, T. A. Kuhlbusch, R. Seuwen, P. Warneck, and P. J. Crutzen, Experimental evaluation of biomass burning emissions: Nitrogen and carbon containing compounds, in *Global Biomass Burning: Atmospheric, Climatic and Biospheric Implications*, edited by J. S. Levine, pp. 289–304, MIT Press, Cambridge, Mass., 1991.

Mahieu, E., C. P. Rinsland, R. Zander, P. Demoulin, L. Delbouille, and G. Roland, Vertical column abundances of HCN deduced from ground-based infrared solar spectra: Long-term trend and variability, *J. Atmos. Chem.*, *20*, 299–310, 1995.

Manning, M. R., C. A. Brenninkmeijer, and W. Allan, Atmospheric carbon monoxide budget in the southern hemisphere: Implications of $^{13}C/^{12}C$ measurements, *J. Geophys. Res.*, *102*, 10,673–10,682, 1997.

Matsueda, H., H. Y. Inoue, M. Ishii, and Y. Tsutsumi, Large injection of carbon monoxide into the upper troposphere due to intense tropical biomass burning in 1997, *J. Geophys. Res.*, *104*, 26,867–26,879, 1999.

McKeen, S. A., S. C. Liu, E.-Y. Hsie, X. Lin, J. D. Bradshaw, S. Smyth, G. L. Gregory, and D. R. Blake, Hydrocarbon ratios during PEM-West A: A model perspective, *J. Geophys. Res.*, *101*, 2087–2109, 1996.

Meier, A., G. C. Toon, C. P. Rinsland, and A. Goldman, Spectroscopic atlas of atmospheric microwindows in the middle infra-red, Atmos. Res. Programme, Swed. Inst. of Space Phys., Kiruna, Sweden, 1997.

Merrill, J. T., Trajectory results and interpretation for PEM-West A, *J. Geophys. Res.*, *101*, 1679–1690, 1996.

Notholt, J., G. C. Toon, C. P. Rinsland, N. S. Pougatchev, N. B. Jones, B. J. Connor, R. Weller, M. Gautrois, and O. Schrems, Latitudinal variations of trace gas concentrations in the free troposphere measured by solar absorption spectroscopy during a ship cruise, *J. Geophys. Res.*, *105*, 1337–1349, 2000.

Novelli, P. C., K. A. Masarie, and P. M. Lang, Distribution and recent changes of carbon monoxide in the lower troposphere, *J. Geophys. Res.*, *103*, 19,015–19,033, 1998.

Olson, J. R., B. A. Baum, D. R. Cahoon, and J. H. Crawford, Frequency and distribution of forest, savanna, and crop fires over tropical regions during PEM-Tropics A, *J. Geophys. Res.*, *104*, 5865–5876, 1999.

Pak, B. C.-Y., Vertical structure of atmospheric trace gases over southeast Australia, Ph.D. thesis, Sch. of Earth Sci., Univ. of Melbourne, Parksville, Victoria, Australia, 2000.

Pougatchev, N. S., B. J. Connor, and C. P. Rinsland, Infrared measurements of the ozone vertical distribution above Kitt Peak, *J. Geophys. Res.*, *100*, 16,689–16,697, 1995.

Pougatchev, N. S., et al., Ground-based infrared solar spectroscopic measurements of carbon monoxide during 1994 Measurement of Air Pollution From Space flights, *J. Geophys. Res.*, *103*, 19,317–19,325, 1998.

Pougatchev, N. S., G. W. Sachse, H. E. Fuelberg, C. P. Rinsland, R. B. Chatfield, V. S. Connors, N. B. Jones, J. Nothlot, P. C. Novelli, and H. G. Reichle Jr., Pacific Exploratory Mission-Tropics carbon monoxide measurements in historical context, *J. Geophys. Res.*, *104*, 26,195–26,207, 1999.

Predoi-Cross, A., J. P. Bouanich, D. C. Benner, A. D. May, and J. R. Drummond, Broadening, shifting, and line asymmetries in the $2 \leftarrow 0$ band of CO and CO-N_2: Experimental results and theoretical calculations, *J. Chem. Phys.*, *113*, 158–168, 2000.

Prinn, R. G., et al., A history of chemically and radiatively important gases in air deduced from ALE/GAGE/AGAGE, *J. Geophys. Res.*, *105*, 17,751–17,792, 2000.

Rinsland, C. P., A. Goldman, and G. M. Stokes, Identification of atmospheric C_2H_2 lines in the 3230–3340 cm^{-1} region of high resolution solar absorption spectra recorded at the National Solar Observatory, *Appl. Opt.*, *24*, 2044–2046, 1985.

Rinsland, C. P., R. Zander, C. B. Farmer, R. H. Norton, and J. M. Russell III, Concentrations of ethane (C_2H_6) in the lower stratosphere and upper troposphere and acetylene (C_2H_2) in the upper troposphere deduced from Atmospheric Trace Molecule Spectroscopy/Spacelab 3 spectra, *J. Geophys. Res.*, *92*, 11,951–11,964, 1987.

Rinsland, C. P., N. B. Jones, and W. A. Matthews, Infrared spectroscopic measurements of the total column abundance of ethane (C_2H_6) above Lauder, New Zealand, *J. Geophys. Res.*, *99*, 25,941–25,945, 1994.

Rinsland, C. P., et al., Northern and southern hemisphere ground-based infrared spectroscopic measurements of tropospheric carbon monoxide and ethane, *J. Geophys. Res.*, *103*, 28,197–28,217, 1998a.

Rinsland, C. P., et al., ATMOS/ATLAS 3 infrared profile measurements of trace gases in the November 1994 tropical and subtropical upper troposphere, *J. Quant. Spectrosc. Radiat. Transfer*, *60*, 891–901, 1998b.

Rinsland, C. P., et al., Infrared solar spectroscopic measurements of free tropospheric CO, C_2H_6, and HCN above Mauna Loa, Hawaii: Seasonal variations and evidence for enhanced emissions from the Southeast Asian tropical fires of 1997–1998, *J. Geophys. Res.*, *104*, 18,667–18,680, 1999.

Rinsland, C. P., E. Mahieu, R. Zander, J. Forrer, and B. Buchmann, Free tropospheric CO, C_2H_6, and HCN above central Europe: Recent measurements from the Jungfraujoch station including the detection of elevated columns during 1998, *J. Geophys. Res.*, *105*, 24,235–24,249, 2000.

Rinsland, C. P., A. Goldman, R. Zander, and E. Mahieu, Enhanced tropospheric HCN columns above Kitt Peak during the 1982–1983 and 1997–1998 El Niño warm phases, *J. Quant. Spectrosc. Radiat. Transfer*, *69*, 3–8, 2001.

Rodgers, C. D., Characterization and error analysis of profiles retrieved from remote sounding measurements, *J. Geophys. Res.*, *95*, 5587–5595, 1990.

Rosen, J., S. Young, J. Laby, N. Kjome, and J. Gras, Springtime aerosol layers in the free troposphere over Australia: Mildura Aerosol Tropospheric Experiment (MATE 98), *J. Geophys. Res.*, *105*, 17,833–17,842, 2000.

Rothman, L. S., et al., The HITRAN molecular spectroscopic database and HAWKS (HITRAN atmospheric workstation): 1996 edition, *J. Quant. Spectrosc. Radiat. Transfer*, *60*, 665–710, 1998.

Rudolph, J., The tropospheric budget and distribution of ethane, *J. Geophys. Res.*, *100*, 11,369–11,381, 1995.

Schoeberl, M. R., and L. C. Sparling, Trajectory modeling, in *Diagnostic Tools in Atmospheric Physics: Proceedings of S.I.F Course CXVI*, edited by G. Fiocco and G. Visconti, North-Holland, New York, 1994.

Smyth, S. B., et al., Factors influencing the upper free tropospheric distribution of reactive nitrogen during the TRACE-A experiment, *J. Geophys. Res.*, *101*, 24,165–24,186, 1996.

Smyth, S., et al., Characterization of the chemical signatures of air masses observed during the PEM experiments over the western Pacific, *J. Geophys. Res.*, *104*, 16,243–16,254, 1999.

Takacs, L. L., A. Molod, and T. Wang, Documentation of the Goddard Earth Observing System (GEOS) general circulation model, *NASA Tech. Memo.*, *104606*, *1*, 1994.

Watson, C. E., J. Fishman, and H. G. Reichle Jr., The significance of biomass burning as a source of carbon monoxide and ozone in the southern hemisphere tropics: A satellite analysis, *J. Geophys. Res.*, *95*, 16,443–16,450, 1990.

Zhao, Y., Y. Kondo, F. J. Murcray, X. Liu, M. Koike, H. Irie, K. Strong, K. Suzuki, M. Sera, and Y. Ikegami, Seasonal variations of HCN over northern Japan measured by ground-based infrared solar spectroscopy, *Geophys. Res. Lett.*, *27*, 2085–2088, 2000a.

Zhao, Y., Y. Kondo, K. Strong, K. Suzuki, M. Sera, and Y. Ikegami, Spectroscopic measurements of tropospheric CO, C_2H_6, and HCN in Japan, in *Proceedings of XVIV Quadrennial Ozone Symposium*, Hokkaido Univ., Sapporo, Japan, 2000b.

L. S. Chiou, Wyle Laboratories, 3300 Macgruder Blvd., Hampton, VA 23666, USA. (chioul@scatmos.larc.nasa.gov)

D. W. T. Griffith and A. Meier, Department of Chemistry, University of Wollongong, Northfields Avenue, Wollongong, N.S.W. 2522, Australia. (david_griffith@uow.edu.au; arndt@uow.edu.au)

C. P. Rinsland (corresponding author), NASA Langley Research Center, Mail Stop 401A, Hampton, VA 23681-2199, USA. (c.p.rinsland@larc.nasa.gov)

(Received December 28, 2000; revised May 4, 2001;
accepted May 18, 2001.)